Proceedings of CONF-APMM 2026 Symposium: Quantum Communication and Model Simulation
DOI: 10.54254/2753-8818/2026.GL35796

Carrier Transport and Recombination Mechanisms in PN Junctions and Applications in Semiconductor Optoelectronic Devices

Qianyun Yu

College of Physics, Qingdao University, Qingdao, China
yuqianyun@qdu.edu.cn

Abstract. PN junctions are one of the most fundamental physical structures in semiconductor optoelectronics. Their operation is governed by carrier diffusion, drift, depletion region formation, built-in electric fields and electron-hole recombination. This review focuses on the carrier transport and recombination mechanisms in PN junctions and discusses how these mechanisms determine the performance of semiconductor optoelectronic devices. Firstly, the fundamental physics of PN junction formation, energy-band bending and bias-dependent carrier injection is summarized. Then, major transport processes including drift-diffusion transport, minority-carrier injection and doping-dependent current behavior are reviewed. Particular attention is paid to radiative recombination and different types of non-radiative recombination. The review further analyzes the effect of PN junctions in light-emitting diodes, solar cells and photodetectors. Finally, emerging research directions, including heterojunction design, interface passivation, low-dimensional semiconductor junctions and integrated optoelectronic devices, are discussed. This review provides a systematic outline for understanding the relationship between the PN-junction and optoelectronic device performance.

Keywords: PN junction, carrier transport, LED, solar cell, photodetector

1. Introduction

The PN junction forms the foundation of contemporary semiconductor devices. It is also a core pillar that supports the development of electronic technology. The PN junction is constructed by the connection of p-type semiconductor and n-type semiconductor. Prior to contact, the Fermi levels in the p-type and n-type regions differ. Upon junction formation, the Fermi level aligns across the entire structure under thermal equilibrium, giving rise to band bending. The charge carriers undergo diffusion due to the concentration difference at the two ends of the PN junction. This carrier redistribution results in the formation of a depletion region and concomitant band bending. The structure of the PN junction decides its unique property. For example, in electroluminescence process, the radiative recombination of injected electrons and holes leads to the emission of photons in forward bias. In the photovoltaic conversion process, electron–hole pairs are generated and then driven apart by the built-in electric field. This process generates electrical power which can be

© 2026 The Authors. This is an open access article distributed under the terms of the Creative Commons Attribution License 4.0 (https://creativecommons.org/licenses/by/4.0/).

DOI: 10.54254/2753-8818/2026.GL35796

extracted from the device. In photodetection, photogenerated carriers can be collected by same built-in field. This process generates measurable photocurrent.

Carrier transport determines how effectively electrons and holes are injected, separated and collected, while recombination determines whether the stored electronic energy is converted into light, electricity or heat. Different optoelectronic applications prioritize different carrier transport and recombination processes within the PN junction. In LEDs, radiative recombination is useful because it produces photons efficiently. However, non-radiative recombination is a process generates excess heat and reduces luminous efficiency. In solar cells, recombination is usually a loss pathway because photogenerated carriers must be collected before recombination occurs. In photodetectors, rapid carrier separation and low dark current are essential for high responsivity and detectivity.

This review focuses on the carrier transport and recombination mechanisms in PN junctions. It then describes their applications, including light-emitting diodes (LEDs), solar cells and photodetectors. Finally, some challenges and outlooks will be discussed in the final section.

2. The carrier transport and recombination mechanisms in PN junctions

2.1. Basic physical mechanisms

The conductivity of doped semiconductors is determined by impurity atoms. These atoms can be categorized to donor impurities and acceptors impurities. When donor impurities are doped in pure semiconductor, it leaves excess negative charged electrons in the conduction band. It makes semiconductor become n-type. By contrast, when acceptor impurities are doped, it leaves excess positive charged holes in the valence band. It makes semiconductor become p-type. Thus, holes dominate carrier transport in the p-type region, with electrons acting as minority carriers. Conversely, electrons are the dominant carriers in the n-type region, whereas holes are present as minority carriers.

The concentration of electrons and holes can be obtained by equation (1) and (2). E_C , E_V and E_F represent the conduction-band minimum (CBM), the valence-band maximum (VBM), and the Fermi energy level respectively.

$$n = N_C exp\left(-\frac{E_C - E_F}{kT}\right) \tag{1}$$

$$p = N_V exp\left(-\frac{E_F - E_V}{kT}\right) \tag{2}$$

This is the classical result under the Boltzmann approximation. N_C and N_V denote the effective densities of states in the conduction and valence bands respectively. Their values are determined by the effective masses of electrons and holes. Equating (1) and (2) under intrinsic conditions yields the intrinsic Fermi level in (3).

DOI: 10.54254/2753-8818/2026.GL35796

$$E_i = \frac{E_C + E_V}{2} + \frac{kT}{2} ln\left(\frac{N_V}{N_C}\right) \tag{3}$$

$$np = n_i^2 \tag{4}$$

For an intrinsic semiconductor, the Fermi level is positioned around the middle of the bandgap. According to mass-action law (4). n_i refers to intrinsic carrier density, which is the equilibrium concentration of electrons or holes generated by thermal excitation in a pure intrinsic semiconductor. For a p-type semiconductor, the concentration of holes is nearly identical to the acceptor concentration (N_A) due to each acceptor introduces one hole. Therefore, the concentration of electrons can be presented.

$$n = \frac{n_i^2}{p} = \frac{n_i^2}{N_A} \tag{5}$$

Because holes concentration is greater than electrons concentration in p-type semiconductor, the Fermi level is lower than middle of bandgap and is located close to the valence band.

$$p = N_V exp\left(-\frac{E_F - E_V}{kT}\right) > N_C exp\left(-\frac{E_C - E_F}{kT}\right) = n \tag{6}$$

$$E_F < \frac{E_C + E_V}{2} \tag{7}$$

Since each donor atom contributes one electron in the n-type semiconductor, the electron concentration is approximately equal to the donor concentration N_D . Similarly, the concentration of holes can be presented.

$$p = \frac{n_i^2}{n} = \frac{n_i^2}{N_D} \tag{8}$$

Because electrons are the majority carriers in an n-type semiconductor, the Fermi level is positioned nearer the conduction band and is higher than middle of bandgap [1].

$$p = N_V exp\left(-\frac{E_F - E_V}{kT}\right) < N_C exp\left(-\frac{E_C - E_F}{kT}\right) = n \tag{9}$$

DOI: 10.54254/2753-8818/2026.GL35796

$$E_F > \frac{E_C + E_V}{2} \tag{10}$$

Prior to forming the junction, the p-type and n-type semiconductors are electrically neutral. Once the p-type and n-type regions are joined, electrons move from the n-type side into the p-type side, while holes travel in the reverse direction. Then electrons and holes recombine together, which quickly depletes the number of carriers in contact region. As a result, electrons left the n-type region near the junction, leaving positive charged donor ions. Holes left the p-type region near the junction, leaving negative charged acceptor ions. Donor ions and acceptor ions cannot diffuse because they are fixed in lattice. Therefore, this region contains almost no mobile charged carriers but consists of immobile charged ions. This is the formation of depletion region and the built-in electric field. The built-in potential also changes along the variation of built-in electric field. Assuming that the PN junction is one-dimensional. And PN junction can be divided to three regions: p-type region, depletion region (from - x_p to x_n) and n-type region. Figure 1 provides the meanings represented by different symbols. The depletion approximation assumes negligible concentrations of free electrons and holes. Therefore, the charge is solely provided by ionized impurities. Poisson's equation can be used to determine the length of the depletion region.

$$W = x_n + x_p = \sqrt{\frac{2\varepsilon_s}{q} \bullet \frac{N_A N_D}{N_A + N_D} V_{bi}} \tag{11}$$

In this expression, W is the depletion region width and V_{bi} is the built-in potential. ε_s denotes the permittivity of the semiconductor, q represents the elementary charge, N_A and N_D correspond to the acceptor and donor concentrations. Equation (11) shows that in asymmetric junctions, W varies with the square root of the built-in potential and is primarily controlled by the more lightly doped side.

Under thermal equilibrium, drift current and diffusion current satisfy the equations below:

$$J_{drift} + J_{diffusion} = 0 \tag{12}$$

$$J_{drift} = q\mu_n n\varepsilon \tag{13}$$

$$J_{diffusion} = \mu_n \frac{kT}{q} \bullet \frac{dn}{dx} \tag{14}$$

Built-in potential can be inferred from these equations.

DOI: 10.54254/2753-8818/2026.GL35796

$$V_{bi} = \frac{kT}{q} ln\left(\frac{N_A N_D}{n_i^2}\right) \tag{15}$$

The built-in potential is generated by the space charge formed during carrier diffusion, resulting in an internal electric field that counteracts further diffusion. Under thermal equilibrium, a constant Fermi level is established across the junction, while band bending occurs in both the conduction and valence bands near the interface.

The voltage V applied across the PN junction affects the width of the depletion region. Therefore, equation (11) should turn into (16):

$$W = x_n + x_p = \sqrt{\frac{2\varepsilon_s}{q} \bullet \frac{N_A N_D}{N_A + N_D}\left(V_{bi} - V\right)} \tag{16}$$

Under forward bias, the number of V is positive. Thus, the potential barrier is lowered and the depletion region becomes narrower, allowing majority carriers to be injected across the junction. Under reverse bias, the number of V is negative. Hence, the potential barrier increases and the depletion region becomes wider, suppressing majority-carrier diffusion while allowing minority-carrier drift. The characteristic of forward bias includes: enhanced carrier injection, exponential increase in current and increased recombination near or beyond the junction region. While the characteristic of reverse bias includes small reverse saturation current, stronger electric field in the depletion region and possible avalanche or Zener breakdown at high voltage. These comparisons between forward and reverse bias provide the basis for understanding rectification, photodiode operation and junction breakdown [2].

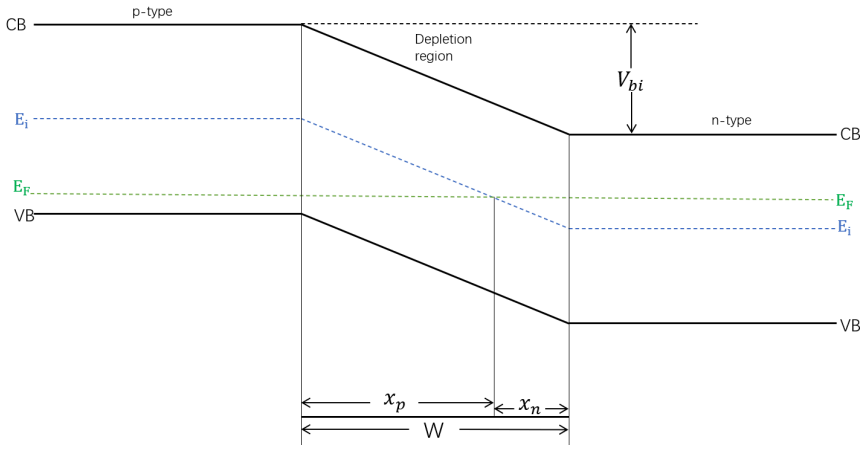

Figure 1. The meaning of each symbol in the PN junction

2.2. Carrier transport mechanisms

Carrier transport in the PN junction is principally attributed to diffusion arising from concentration gradients and drift driven by the internal electric field. The relative importance of these two processes depends on the bias condition, material properties, doping profile and device structure.

DOI: 10.54254/2753-8818/2026.GL35796

Table 1 describes the differences among various transport mechanisms. Equation (17) describes the total current density arising from both electrons and holes.

$$\begin{cases} J_n = q\mu_n n\varepsilon + qD_n \frac{dn}{dx} \\ J_p = q\mu_p p\varepsilon + qD_p \frac{dp}{dx} \end{cases} \tag{17}$$

These two equations are called the drift-diffusion equations. μ_n and μ_p is mobility of electrons and holes respectively. D_p and D_n respectively represent the diffusion coefficients of holes and electrons. The first term in both equations represents the contribution of drift current. The drift current is influenced by carrier concentration, mobility and the strength of the electric field. Drift transport becomes the predominant carrier transport process inside the depletion region due to the presence of a strong built-in electric field. Especially under reverse bias conditions, the diffusion process is inhibited. Thus, drift current becomes the main mode of transport in reverse bias. It is also a better opportunity to rapidly separate and collect photogenerated carriers. Then the second item represents the contribution of diffusion. When there is a concentration difference of charge carriers within a semiconductor, charge carriers tend to migrate from areas with higher concentrations toward areas with lower concentrations. Under forward bias conditions, a large number of majority carriers are injected into the opposite region, thereby forming minority carriers. Therefore, the diffusion process becomes the main contributor to the forward current. Equation (17) is the fundamental equation that serves as the basis for analyzing the carrier transport behavior of PN junctions, solar cells, LEDs and photodetectors [3]. Einstein's relation (18) links the diffusive and drift transport coefficients under thermal equilibrium [1].

$$\frac{D_n}{\mu_n} = \frac{D_p}{\mu_p} = \frac{kT}{q} \tag{18}$$

Table 1. The differences among various transport mechanisms

Transport mechanism	Physical driving force	Dominant region/condition	Device implication
Diffusion	Carrier concentration gradient	Quasi-neutral regions; forward bias	Determines injected minority-carrier profile and forward current
Drift	Electric field	Depletion region; reverse bias	Enables rapid separation and collection of photogenerated carriers
Thermionic emission	Thermal excitation over a barrier	Heterojunctions and Schottky-like contacts	Affects barrier-limited current and temperature dependence
Tunneling	Quantum-mechanical barrier penetration	Highly doped or narrow depletion regions	Important in Zener breakdown and tunnel junctions

Diode equation describes the current-voltage behavior of an ideal PN junction. In actual devices, deviations arise from series resistance, shunt leakage, interface states, high-level injection and recombination in the depletion region.

DOI: 10.54254/2753-8818/2026.GL35796

$$I = I_0(e^{\frac{qV}{nkT}} - 1) \tag{19}$$

In equation (19), V represents the externally applied bias voltage. I_0 corresponds to the saturation current. n denotes the ideality factor [4]. The current in the PN junction is growing exponentially in forward bias. While in reverse bias, the current is nearly constant. Ideality factor close to 1 usually indicates diffusion current dominance in neutral region. The recombination current accounts for the majority in the depletion region when ideality factor close to 2. At high forward current, series resistance causes deviation from the ideal exponential relationship. At reverse bias, leakage current and breakdown behavior reveal defect density and electric-field distribution. Under forward bias, most charge carriers will cross the barrier and enter the opposite region. For example, electrons and holes are injected into the p-type region the n-type region respectively. Minority-carrier lifetime and diffusion length play key roles in governing their transport and recombination.

$$L_n = \sqrt{D_n \tau_n}, \quad L_p = \sqrt{D_p \tau_p} \tag{20}$$

L_n and L_p are electrons diffusion length and holes diffusion length re spectively. τ_n and τ_p are electrons lifespan and holes lifespan respectively. A longer diffusion length benefits solar cells by enabling photogenerated carriers to reach the depletion region before recombining. In LEDs, the injected carrier lifetime and confinement determine the spatial distribution of radiative recombination [3].

2.3. Recombination mechanisms

Recombination refers to the annihilation of an electron–hole pair. The released energy appears as photon emission, phonon generation or energy transfer to another carrier. Whether the recombination process is beneficial or detrimental depends on the function of the device.

During radiative recombination, an electron from the conduction band recombines with a hole in the valence band and releases a photon. The wavelength of photon is approximately determined by the bandgap energy.

$$\lambda = \frac{hc}{E_g} \tag{21}$$

Materials possessing a direct bandgap, including GaAs, InP and GaN, exhibit superior performance for light emission. Radiative recombination is central to LEDs and laser diodes. By contrast, it is not usually desired in solar cells unless radiative-limit analysis is considered.

The mechanisms described below—Shockley–Read–Hall (SRH), Auger and surface/interface recombination—are collectively classified as non-radiative recombination. SRH recombination is a defect-assisted non-radiative mechanism. Trap states located within the bandgap capture carriers and provide intermediate energy levels for recombination. Recombination occurs most efficiently

DOI: 10.54254/2753-8818/2026.GL35796

through deep-level traps which situated near the midgap energy. Equation (22) express the SRH recombination rate.

$$R_{SRH} = \frac{n_p - n_i^2}{\tau_p \left(n + n_1\right) + \tau_n \left(p + p_1\right)} \tag{22}$$

SRH recombination reduces minority-carrier lifetime and diffusion length. It is strongly related to crystal defects, impurities, dislocations, grain boundaries and interface states. In solar cells, SRH recombination lowers open-circuit voltage and conversion efficiency. In photodetectors, it contributes to dark current and noise. In LEDs, it reduces internal quantum efficiency, especially at low current density [5, 6].

In Auger recombination, the recombination energy of an electron–hole pair is transferred to another charge carrier instead of being emitted radiatively. This mechanism becomes important under high carrier density, high injection or heavy doping conditions. Its rate often increases strongly with carrier concentration, making it a major loss mechanism under high injection.

$$R_{Auger} = C_n n^2 p + C_p p^2 n \tag{23}$$

C_n and C_p are Auger coefficient. Therefore, Auger recombination can contribute to efficiency droop in high-power LEDs. It also limits the performance of highly doped junctions and high-concentration photovoltaic devices [3].

Surface and interface recombination becomes increasingly important in thin-film, nanostructured and heterojunction devices. Dangling bonds, interfacial defects, lattice mismatch and chemical instability may introduce states that act as recombination centers. The greater the surface recombination rate, the more readily the charge carriers are lost at the surface. In order to curb such recombination losses, surface passivation is introduced to reduce dangling-bond-related recombination. And buffer layers are used to reduce lattice mismatch and interface defect density. Interface engineering is especially important in heterojunction solar cells, quantum-well LEDs and two-dimensional semiconductor junctions. The following table illustrates the differences among various recombination mechanisms. Table 2 compares different recombination types from physical origin, dominant condition to main influence on devices.

Table 2. The differences between various recombination types

Recombination type	Physical origin	Dominant condition	Main influence on devices
Radiative recombination	Direct electron-hole recombination with photon emission	Direct-bandgap materials and well-confined active regions	Useful for LEDs and lasers; may define radiative efficiency limit
Shockley-Read-Hall recombination	Trap-assisted recombination through defect levels	Defective bulk, grain boundaries, interfaces	Reduces lifetime, increases dark current, lowers efficiency
Auger recombination	Energy transferred to a third carrier	High carrier density, high injection, heavy doping	Causes high-injection loss and efficiency droop

DOI: 10.54254/2753-8818/2026.GL35796

Table 2. (continued)

Surface/interface recombination	Dangling bonds and interface states	Nanostructures, thin films, heterojunctions	Increases leakage, noise and non-radiative loss

3. Applications

3.1. LED

The fundamental role of a light-emitting diode (LED) is the conversion of electrical energy into optical energy. Its working principle can be summarized as follows. Under forward bias, the applied electric field lowers the potential barrier across the depletion region of the PN junction. It facilitates the injection of electrons and holes. Within the active region, these carriers undergo radiative recombination and emit photons. Then the generated photons are emitted from the PN junction and extracted by the device structure. LED must use direct bandgap semiconductors. Because electron transitions from the conduction band to the valence band occur without the involvement of phonons. The probability of radiation recombination occur in direct bandgap semiconductors is much higher than that in indirect bandgap materials. Therefore, efficient electroluminescence can be achieved [3].

In 2023, Cao et al. used a template made of porous alumina membranes. The pore size on the template is ultra-small. A generic solution-based approach, which is free of both organic ligands and anti-solvents, was employed to fabricate crystalline all-inorganic perovskite quantum wire arrays. This wire arrays have ultrahigh density and uniformity. Benefiting from strong quantum confinement and efficient light out-coupling, the perovskite quantum wire arrays exhibited a high photoluminescence quantum yield (PLQY), making them suitable for blue, sky-blue, green and pure-red LEDs. When this quantum wires arrays were applied in LED, Cao et al. also added a dual-functional small molecule. The molecule functions as a surface passivation agent, a hole-transporting material and a healing agent for halide vacancies. Finally, they achieved spectrally stable electroluminescence LED devices with the color as mentioned before. The external quantum efficiencies (EQE) of the LEDs in each color are 12.41%, 16.49%, 26.09% and 9.97% respectively. In conclusion, these measures suppressed non-radiative recombination and achieved record external quantum efficiency [7].

In 2024, Yuan et al. created efficient blue perovskite LEDs with a mixed 2D-3D perovskite and a multifunctional ionic additive. It allows the regulation of reduced-dimensional phases, suppress non-radiative recombination and maintain spectral stability. Efficient electroluminescence is achieved in a series of devices based on mixed bromide/chloride quasi-3D regions. The maximum EQE reached 21.4% and the operational stability increased by thirty times compared with control LED. It proves the precise control of carrier transport and recombination in PN junctions is essential for high-performance blue LEDs [8].

3.2. Solar cells

Solar cells operate by converting optical energy into electrical energy. During this process, the semiconductor absorbs photons with energies higher than the bandgap energy.

$$I(x) = I_0 \cdot e^{-\alpha(\lambda)\cdot x} \tag{24}$$

DOI: 10.54254/2753-8818/2026.GL35796

$\alpha(\lambda)$ is the absorption coefficient. This equation reveals that the light intensity decays exponentially with the penetration depth. The absorption process creates electron-hole pairs, while the remaining energy above the bandgap is released in the form of heat through thermalization. The built-in electric field formed within the depletion region provides the driving force necessary for the transport of electrons and holes. The separation of electrons and holes by the built-in electric field occurs much faster than their recombination. Therefore, they move respectively to the N-region and the P-region before undergo recombination. The separated carriers are collected by the metal electrodes or the selective contact layer and then transported to the external circuit. Finally, photocurrent occurs in external circuit [9].

In 2025, highly effective and mechanically stable and bendable perovskite heterojunction monolithic tandem solar cells were successfully created by Sun et al. They improved charge transfer across all interfaces and mitigated residual interfacial stress by maintaining high phase homogeneity. The power conversion efficiency (PCE) of solar cells was up to 29.88%. It outperformed other kinds of flexible solar devices based on perovskite. These improvements facilitate carrier transport across the heterojunction PN interface and improve carrier collection [10].

In 2025, Wang et al. also reported a significant progress of solar cells. They introduced reactive-plasma-deposited (RPD) cerium and hydrogen co-doped indium oxide (ICO:H) to fabricate the recombination layer. This improves self-assembled monolayers (SAMs) coverage and interfacial charge transfer. The flexible perovskite/crystalline silicon (c-Si) tandem solar cell made by Wang et al. have 33.6% efficiency and a record high open-circuit voltage (Voc) of 2.015 V. Despite undergoing numerous bends, it still maintains its original high efficiency. It also exhibited extraordinary operational and damp-heat stability. The optimized interface promotes more efficient carrier transport through the tandem PN junction [11].

3.3. Photodetector

A photodetector refers to a semiconductor device designed to convert optical signals into electrical signals. Photons incident on the semiconductor with energies exceeding the bandgap are absorbed by the material. Therefore, the selection of semiconductor materials determines the working wavelength range of the detector. Narrow-bandgap materials (InGaAs, HgCdTe) are used for infrared detection. Wide-bandgap materials (GaN, SiC) are used for ultraviolet detection. Silicon and InP are capable of operating across the visible and near-infrared spectral regions. The process of photons absorption generates electron–hole pairs. This process is controlled by equation (24). Thus, Photons with shorter wavelengths are absorbed close to the front surface, whereas those with longer wavelengths penetrate further into the material. Photodetector works in reverse bias or zero bias. In this situation, the depletion region is significantly widened. The built-in electric field intensity increases proportionally. The strong electric field rapidly separates photogenerated carriers which are created in or close to the depletion region. Electrons move toward the N-region, whereas holes drift toward the P-region. The drift time is significantly less than the carrier recombination time. The separated charge carriers are extracted by the electrodes, generating an electric current in the external circuit [3].

In 2025, A photodetector, which can distinguish different frequencies, was created in a single device by Ming et al. They linked two opposing, equal electromotive forces. Then the output of this device is close to zero in constant light illumination. To adjust the frequency that the gadget detected, they employed an asymmetric 2D–3D–2D perovskite structure. The reaction times of the reverse photodiodes varyed. As a result, the device exhibited a response only in the vicinity of a certain frequency. It is possible to change the 2D perovskite components to manipulate frequency.

DOI: 10.54254/2753-8818/2026.GL35796

Within the frequency-dependent photoresponse range of 0.8–9.7 MHz, a highly rapid response time of 19.7/18.3 ns was exhibited in the target device. The device relies on efficient separation and collection of photogenerated carriers in reverse-biased PN junctions [12].

Yoshioka et al. reported a gate-tunable graphene photodetector capable of achieving a bandwidth as high as 220 GHz in 2022. They employed a resistive zinc oxide top gate to lower the RC time constant. The photocurrent from electrode is extracted very instantly. It features an extremely short carrier transit time through the graphene channel, which is several micrometers in length. This phenomenon follows the Shockley–Ramo theorem. Photocurrent generation time is remarkably adjustable, ranging from instantaneous to more than 4 ps. Its origin can be attributed to intraband carrier–carrier scattering determined by the Fermi level. The improved carrier extraction contributes to the ultrafast response of the PN-junction photodetector [13].

4. Challenges and outlook

4.1. Challenges

A major challenge in PN-junction optoelectronic devices is the suppression of non-radiative recombination. This requires improved crystal quality, defect passivation, interface engineering, optimized growth processes and balanced carrier injection.

In the field of advanced heterojunction design, electron-blocking and hole-blocking layers can improve carrier confinement. This prevents the injected electrons or holes from escaping from the active region. Selective contacts in solar cells can reduce recombination while maintaining carrier extraction. Tunnel junctions can connect multiple sub-cells in multi-junction optoelectronic devices. Band offset engineering can enhance charge separation or radiative recombination depending on device purpose.

Low-dimensional systems, including two-dimensional semiconductors, nanowires and quantum dots, provide new opportunities for PN junction design. However, they also present challenges in controllable doping, contact resistance, surface recombination and large-area fabrication.

In emerging optoelectronic applications, micro-LEDs require strong current spreading, low defect density and efficient light extraction to overcome the challenges posed by size reduction. Quantum-dot LEDs introduce carrier confinement and size-dependent emission but require surface control. Perovskite and organic-inorganic hybrid junctions require stability improvement and defect management. Near-infrared photodetectors and integrated photonics demand low dark current and high-speed carrier extraction.

4.2. Outlooks

There are still some issues with the current development of PN junctions Firstly, achieving high carrier mobility while simultaneously suppressing recombination loss remains a critical challenge in advanced PN junctions. Secondly, quantitatively separating the contributions of SRH, Auger and surface recombination in practical devices remains experimentally challenging. It is also important to fabricate low-defect, low-resistance heterojunction interfaces at scale. In addition, conventional PN-junction theory needs to be extended to quantum dots, two-dimensional materials and perovskite semiconductors. Lastly, device stability needs to be improved while maintaining high efficiency under high current density or strong illumination. As materials synthesis and device engineering continue to advance, these challenges are expected to be gradually overcome.

DOI: 10.54254/2753-8818/2026.GL35796

5. Conclusion

The PN junction is the most fundamental structure of semiconductor optoelectronic devices. A depletion region and built-in electric field are created by this special structure. They determine the direction of carrier transport in PN junctions. By varying the external bias, the depletion region width and carrier injection level can be precisely controlled. Forward bias promotes electron-hole recombination in the depletion region. By contrast, reverse bias enables the strong built-in electric field to efficiently separate photogenerated electron-hole pairs.

Carrier transport is dominated by drift, diffusion, injection and collection processes. Diffusion current is generated by carrier concentration difference and dominates in forward bias. It also enables adequate carriers to be injected under forward bias. Drift current is driven by the electric field and becomes the dominant current component in reverse biased depletion regions. As a result, it ensures that electrons and holes are separated in the depletion region. Then the carriers are driven to the electrodes and collected, generating current in the external circuit.

Carrier recombination can be divided into radiative recombination and non-radiative recombination. The latter category includes SRH, Auger and surface/interface recombination. Photons are produced through radiative recombination. This is the process necessary for achieving high luminous efficiency in LEDs. SRH recombination derives from lattice defects. Auger recombination is caused by high carrier concentration. Surface and interface recombination usually result from dangling bonds, interface defects and lattice mismatch. Therefore, recombination can be controlled by understanding the different mechanisms of these processes.

Different optoelectronic devices have different optimization goals. Enhancing radiative recombination and restraining non-radiative recombination is the core goal of LED design. Direct-bandgap materials are also a fundamental requirement of LED. High PLQY and EQE are achieved by surface passivation, reducing crystal defects and introducing multiple quantum wells. By contrast, photogenerated charge carriers should be rapidly separated and collected before recombination occurs in solar cells and photodetectors. In solar cells, high PCE is achieved through surface passivation, enhanced light trapping and multi-junction/tandem architectures. In photodetectors, common strategies include employing a broad depletion region (e.g. PIN structures), increasing reverse bias voltage and strictly suppressing the dark current, all of which contribute to high responsivity and quantum efficiency.

The future development of PN junction will rely more on the collaborative optimization of materials and device structures. Defects should be reduced by various methods. Carrier transport efficiency should be improved through band alignment engineering. Furthermore, two-dimensional materials, quantum dots, nanowires and other low-dimensional PN junction structures will provide new development directions for high-performance and miniaturized optoelectronic devices.

References

[1] Sze, S. M., Li, Y., & Ng, K. K. (2021). *Physics of semiconductor devices*. John Wiley & Sons, Hoboken, NJ, USA.
[2] Shockley, W. (1949). The theory of p–n junctions in semiconductors and p–n junction transistors. *Bell System Technical Journal, 28*(3), 435–489. DOI: 10.1002/j.1538-7305.1949.tb03645.
[3] Streetman, B. G., & Banerjee, S. (2000). *Solid state electronic devices*. Prentice Hall, Upper Saddle River, NJ, USA.
[4] Sah, C. T., Noyce, R. N., & Shockley, W. (1957). Carrier generation and recombination in pn junctions and pn junction characteristics. *Proceedings of the IRE, 45*(9), 1228–1243. DOI: 10.1109/JRPROC.1957.278528.
[5] Shockley, W., & Read, W. T., Jr. (1952). Statistics of the recombinations of holes and electrons. *Physical Review, 87*(5), 835. DOI: 10.1103/PhysRev.87.835.

DOI: 10.54254/2753-8818/2026.GL35796

[6] Hall, R. N. (1952). Electron-hole recombination in germanium. *Physical Review, 87*(2), 387. https://doi.org/10.1103/PhysRev.87.387
[7] Cao, Y. B., Zhang, D., Zhang, Q., et al. (2023). High-efficiency, flexible and large-area red/green/blue all-inorganic metal halide perovskite quantum wires-based light-emitting diodes. *Nature Communications, 14*, Article 4611. https://doi.org/10.1038/s41467-023-40348-4
[8] Yuan, S., Dai, L., Sun, Y., et al. (2024). Efficient blue electroluminescence from reduced-dimensional perovskites. *Nature Photonics, 18*(5), 425–431. https://doi.org/10.1038/s41566-024-01415-7
[9] Green, M. A. (1981). *Solar cells: Operating principles, technology and system applications*. Prentice-Hall, Englewood Cliffs, NJ, USA.
[10] Sun, Y., Li, F., Zhang, H., et al. (2025). Flexible perovskite/silicon monolithic tandem solar cells approaching 30% efficiency. *Nature Communications, 16*, Article 5733.
[11] Wang, S., Li, W., Yu, C., et al. (2026). Flexible perovskite/silicon tandem solar cells with 33.6% efficiency. *Nature, 649*(8095), 59–64.
[12] Min, L., Sun, H., Guo, L., et al. (2024). Frequency-selective perovskite photodetector for anti-interference optical communications. *Nature Communications, 15*, Article 2066. https://doi.org/10.1038/s41467-024-46320-2
[13] Yoshioka, K., Wakamura, T., Hashisaka, M., et al. (2022). Ultrafast intrinsic optical-to-electrical conversion dynamics in a graphene photodetector. *Nature Photonics, 16*(10), 718–723. https://doi.org/10.1038/s41566-022-01063-4